Although the discussion so far has focused upon a semi-infinite fluid with no bottom boundary, these ideas extend straightforwardly to interfacial waves in multi-layer fluids that are vertically bounded or unbounded. The dispersion relation and polarization relations are unchanged but the lateral boundary conditions restrict the allowable wavenumbers to $k_n = n\pi/L$ with $n = 1, 2, \ldots$

2.6 Shear flows

So far we have assumed the fluid is stationary in the absence of waves. However, in many geophysical circumstances currents and winds have changing horizontal speed with height. These are shear flows.

For example, the flow of fresh water into the ocean at an estuary could be approximated by a two-layer fluid in which the upper layer moves with uniform speed over stationary saline fluid. In another example that we have seen, the horizontal velocity field of baroclinic waves is oriented in opposite directions on either side of the interface. In some circumstances the shear at the interface can be so strong as to cause the interface to wrap up into vortices.

Here we will derive the equations for interfacial waves in the presence of shear in multi-layered fluids. In certain circumstances we will see that the resulting dispersion relations allow for a complex-valued frequency whose real part is the frequency in the normal sense. If the imaginary part is non-zero, this means the amplitude of the disturbance grows exponentially in time. The derivation and analysis of equations describing such potentially unstable disturbances comprise what is called 'hydrodynamic stability theory'.

The essence of stability theory for temporally growing disturbances is to assess whether complex ω exists for any (real-valued) k and, if so, to determine for what k the growth rate is largest. Spatial instability, in which ω is real and k is complex, and absolute-convective instability, in which both may be complex, are not considered here.

2.6.1 Derivation of equations

For simplicity, here we neglect Coriolis forces and assume the fluid is laterally unbounded, incompressible and two-dimensional, having structure in the x- and z-directions alone. The fluid is composed of n layers, each with uniform density ρ_i for $i = 1 \ldots n$. That is, the background density $\bar{\rho}(z)$ is piecewise-constant. The ambient flow is horizontal, varying only in the vertical. This is referred to as a 'parallel flow'.

In general, we would like to allow vertical shear within a layer, so we cannot assume the fluid is irrotational. Instead we will work with the momentum equations

for an incompressible fluid. The motion of waves results in velocity fluctuations $\vec{u} = (u, w)$ so that the total velocity field is $(\bar{U} + u, w)$. Consistent with linear theory for small-amplitude disturbances, we will assume that the fluctuation quantities are small but that $\bar{U}$ can be large.

Substituting the total velocity in the x-momentum equation of (1.72), setting $f_0 = 0$ and keeping only those terms that are linear in fluctuation quantities (hence, for example, we keep $\bar{U}\,\partial_x u$ but discard $u\partial_x u$ in the advection terms of the material derivative), we find

$$\frac{\partial u}{\partial t} + \bar{U}\frac{\partial u}{\partial x} + w\bar{U}' = -\frac{1}{\bar{\rho}}\frac{\partial p}{\partial x}. \tag{2.127}$$

Here the prime denotes an ordinary z-derivative.

Similarly, the z-momentum equation becomes

$$\frac{\partial w}{\partial t} + \bar{U}\frac{\partial w}{\partial x} = -\frac{1}{\bar{\rho}}\frac{\partial p}{\partial z}. \tag{2.128}$$

These equations apply within each layer of the multi-layer fluid. There is no buoyancy term in (2.128) because within a uniform-density liquid this is balanced by the background hydrostatic pressure. Buoyancy effects are felt through the fluctuation pressure gradient which in turn depends upon the vertical displacement of interfaces that bound each layer.

Because the fluid is incompressible, we can represent the velocity fields by derivatives of the streamfunction, ψ. Separating the background and fluctuation parts, we define the fluctuation streamfunction so that

$$(u, w) = \left(-\frac{\partial \psi}{\partial z}, \frac{\partial \psi}{\partial x}\right). \tag{2.129}$$

This can be substituted into (2.127) and (2.128) to give two equations in the unknown functions ψ and p.

We could combine these to derive a single differential equation for, ψ, say. However, the mathematics is less cumbersome if we first Fourier transform the equations in x and t. This can be done because the coefficients of the equations depend only upon z. Substituting

$$\psi = \hat{\psi}(z)\, e^{\imath(kx-\omega t)} \text{ and } p = \hat{p}(z)\, e^{\imath(kx-\omega t)}, \tag{2.130}$$

the momentum equations become

$$(\bar{U} - c)\hat{\psi}' - \bar{U}'\hat{\psi} = \frac{1}{\bar{\rho}}\hat{p} \tag{2.131}$$

and

$$-k^2(\bar{U}-c)\hat{\psi} = -\frac{1}{\bar{\rho}}\hat{p}'. \tag{2.132}$$

For convenience, we have defined $c \equiv \omega/k$. This is the phase speed of the waves when ω and k are both real-valued.

Assuming that $\bar{\rho}$ is constant in each layer and eliminating $\hat{p}$ from these equations gives Rayleigh's equation

$$\hat{\psi}'' - \left(\frac{\bar{U}''}{\bar{U}-c} + k^2\right)\hat{\psi} = 0. \tag{2.133}$$

This describes the structure of waves everywhere within a slab of fluid of uniform density. In particular, if there is no background flow, then Rayleigh's equation is identical in form to (2.109). Whereas that formula gives the vertical structure of the velocity potential, (2.133) gives the vertical structure of the streamfunction. Both predict that the waves have amplitudes that change exponentially over a vertical e-folding distance k^{-1}.

The coupling between layers is once again determined by interface conditions that require continuity of mass and pressure. These formulae must be written in terms of the streamfunction and must account for changes in the background flow across the interfaces.

For material on the interface to stay there we require $w = D\eta/Dt$ to be continuous, in which η is the vertical displacement of the interface. Linearizing the material derivative, the statement that the vertical displacement at the lower side of the interface is equal to that at the upper side is given by the condition that

$$\frac{\hat{\psi}}{\bar{U}-c} \tag{2.134}$$

is continuous across the interface.

Requiring that the pressure does not jump discontinuously across the interface, we must have continuity of the following quantity:

$$\bar{\rho}\left[(\bar{U}-c)\hat{\psi}' - \bar{U}'\hat{\psi} - \frac{g}{\bar{U}-c}\hat{\psi}\right]. \tag{2.135}$$

This is found through manipulation of the horizontal and vertical momentum equations.

The complete description of small amplitude disturbances in a multi-layer shear flow is given by the ordinary differential equation (2.133) together with interface conditions (2.134) and (2.135), and conditions for boundedness at infinity or no normal flow at rigid upper and lower boundaries.

Table 2.2. *General and special conditions used to match the solutions for the streamfunction amplitude $\hat{\psi}(z)$ across interfaces where the background horizontal velocity, $\bar{U}$, and/or density, $\bar{\rho}$, change. The quantities in the middle and left column must simultaneously hold the same values above and below the interface. The expressions involve $c \equiv \omega/k$, which is the phase speed c_{Px} one would extract from a horizontal time series.*

	Material continuity	Pressure continuity
General	$\hat{\psi}/(\bar{U}-c)$	$\bar{\rho}\left[(\bar{U}-c)\hat{\psi}' - \bar{U}'\hat{\psi} - g/(\bar{U}-c)\hat{\psi}\right]$
$\bar{U}$ continuous	$\hat{\psi}$	$\bar{\rho}\left[(\bar{U}-c)\hat{\psi}' - \bar{U}'\hat{\psi} - g/(\bar{U}-c)\hat{\psi}\right]$
$\bar{\rho}$ continuous	$\hat{\psi}/(\bar{U}-c)$	$(\bar{U}-c)\hat{\psi}' - \bar{U}'\hat{\psi}$
$\bar{\rho}$, $\bar{U}$, $\bar{U}'$ continuous	$\hat{\psi}$	$\hat{\psi}'$
Boussinesq	$\hat{\psi}/(\bar{U}-c)$	$(\bar{U}-c)\hat{\psi}' - \bar{U}'\hat{\psi} - g\bar{\rho}/[\varrho_0(\bar{U}-c)]\hat{\psi}$

The interface conditions can be simplified under special circumstances, summarized in Table 2.2. In particular, if the background density varies continuously, it follows from (2.134) that (2.135) reduces to

$$(\bar{U}-c)\hat{\psi}' - \bar{U}'\hat{\psi}. \tag{2.136}$$

Otherwise, if the density jump is small compared to the characteristic density, ρ_0, then (2.136) reduces to the condition that the following quantity must vary continuously across the interface:

$$(\bar{U}-c)\hat{\psi}' - \bar{U}'\hat{\psi} - \frac{g\bar{\rho}}{\rho_0}\left[\frac{\hat{\psi}}{\bar{U}-c}\right]. \tag{2.137}$$

This is the Boussinesq form of the pressure continuity condition which states that the density jump is only important in its effect upon buoyancy forces.

2.6.2 Rayleigh waves

Analytic solutions of Rayleigh's equation (2.133) are readily found if the background velocity $\bar{U}$ is constant or if it varies linearly with height, in which case $\bar{U}$ prescribes a uniform shear flow. In this case, the $\bar{U}$ dependence vanishes from (2.133) and so the streamfunction amplitude, $\hat{\psi}$, is given by exponential functions.

Though sometimes algebraically cumbersome, we can straightforwardly find analytic solutions for $\hat{\psi}$ and the dispersion relation if $\bar{U}$ is piecewise-linear, meaning that it is subdivided into vertical ranges over which $\bar{U}$ is either constant or varies

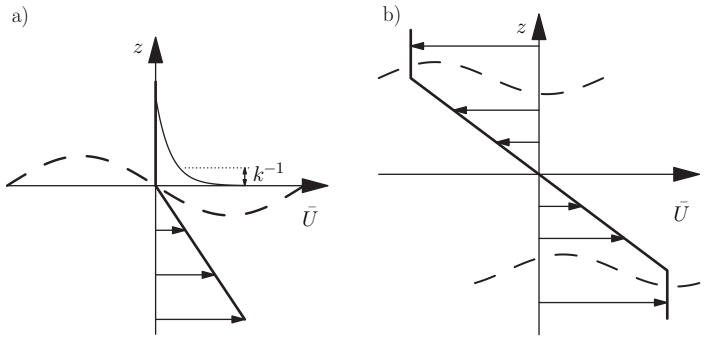

Fig. 2.13. a) Waves associated with a kinked-shear velocity profile. The vertical extent decays exponentially over a distance k^{-1} from the kink and the waves move in the direction of the shear. b) Wave-pairs associated with a shear layer. The waves on the upper flank move rightwards with respect to the upper layer flow; the waves on the lower flank move leftwards with respect to the lower layer flow. The background flow is shown as the solid black line and the waves are illustrated by dashed lines.

linearly with height. In each range we have a pair of exponential solutions which couple from one layer to the next through the interface conditions (2.134) and (2.135).

First we demonstrate this with the simple circumstance of a uniform-density fluid having the following kinked-shear flow profile in an unbounded domain:

$$\bar{U} = \begin{cases} 0 & z \geq 0 \\ -s_0 z & z < 0 \end{cases}, \tag{2.138}$$

in which the shear s_0 below $z = 0$ is constant. This ambient flow field is illustrated in Figure 2.13a.

Requiring bounded solutions to (2.133) gives the streamfunction amplitude in the upper and lower layer:

$$\hat{\psi} = \begin{cases} \mathcal{A}e^{-kz} & z \geq 0 \\ \mathcal{B}e^{kz} & z < 0. \end{cases} \tag{2.139}$$

The interface conditions (2.134) and (2.135) applied at $z = 0$ give the matrix equation

$$\begin{pmatrix} 1 & -1 \\ ck & ck - s_0 \end{pmatrix} \begin{pmatrix} \mathcal{A} \\ \mathcal{B} \end{pmatrix} = \begin{pmatrix} 0 \\ 0 \end{pmatrix}. \tag{2.140}$$

This eigenvalue problem has nontrivial solutions if the determinant of the matrix is zero, that is if $2ck - s_0 = 0$ in which $c = \omega/k$. The structure of the waves is illustrated in Figure 2.13a.

Thus we have determined the dispersion relation for waves that exist due to vertically varying shear:

$$\omega = s_0/2. \tag{2.141}$$

The frequency is independent of wavenumber and the group velocity is zero. Because ω is always real, we have shown that the kinked-shear profile is stable. The phase speed of the waves is $c = s_0/2k$. This matches the speed of the background flow at some vertical level below $z = 0$, and it more closely matches the flow speed at $z = 0$ as k increases and the horizontal and vertical extents of the disturbance decrease.

These waves, driven by shear-induced pressure fluctuations, have no generally accepted name. For convenience here we will describe them as Rayleigh waves, although this terminology should not be confused with that used to describe surface-trapped waves in solids.

2.6.3 Shear layer instability in uniform-density fluid

If $\bar{U}$ describes a flow with uniform shear over a finite depth, it is called a shear layer. Here we will show that a shear layer in uniform density fluid is unstable through resonant coupling between a pair of Rayleigh waves. The process is often referred to as Kelvin–Helmholtz instability, after the two scientists who first examined the phenomenon.

The background flow is prescribed by

$$\bar{U} = \begin{cases} -U_0 & z \geq H \\ -U_0 \frac{z}{H} & |z| < H \\ U_0 & z \leq -H \end{cases}. \tag{2.142}$$

This velocity profile is effectively the result of splicing together two kinked-shear flow profiles of the form (2.138), as shown in Figure 2.13b.

Requiring bounded solutions to (2.133), we find

$$\hat{\psi} = \begin{cases} \mathcal{A}e^{-kz} & z \geq H \\ \mathcal{B}_1 \sinh kz + \mathcal{B}_2 \cosh kz & |z| < H \\ Ce^{kz} & z \leq -H \end{cases}. \tag{2.143}$$

Here the solutions in the middle region have been written in terms of hyperbolic functions in order to take advantage of symmetry as in (2.110) for interfacial waves in a three-layer fluid.

Applying the interface conditions at $z = \pm H$ gives four equations in the four unknowns $\mathcal{A}$, $\mathcal{B}_1$, $\mathcal{B}_2$ and C. Solving the eigenvalue problem gives the dispersion

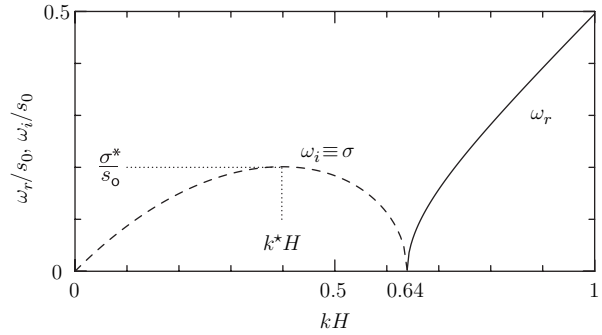

Fig. 2.14. Frequency (ω_r, solid line) and instability growth rate ($\omega_i \equiv \sigma$, dashed line) of horizontally periodic disturbances with wavenumber k superimposed upon an unstratified piecewise-linear shear layer of depth H. For $kH \lesssim 0.64$, $\omega_r = 0$; for $kH \gtrsim 0.64$, $\omega_i = 0$.

relation

$$\omega^2 = \frac{1}{4}{s_0}^2\Big[(1-2kH)^2 - e^{-4kH}\Big], \tag{2.144}$$

in which $s_0 \equiv U_0/H$. The corresponding (complex-valued) dispersion relation is plotted in Figure 2.14 for positive frequency when ω is real and for positive growth rate $\sigma = \omega_i$ when $\omega^2 < 0$.

In the limit $kH \to \infty$, the dispersion relation becomes $\omega \to \pm s_0(1-2kH)/2 = \pm(s_0/2 - U_0 k)$. The positive root corresponds to the dispersion relation (2.141) for Rayleigh waves with a constant flow, $-U_0$, overlying a uniform shear flow. The negative root corresponds to Rayleigh waves with a shear flow overlying a constant flow with speed U_0. Indeed, for large k the vertical extent of the Rayleigh waves at the upper and lower kink in the shear is so small that one disturbance does not feel the influence of the other.

Thus we see that the dispersion relation (2.144) describes the co-existence of a pair of Rayleigh waves that couple together when their horizontal and vertical extent, k^{-1}, is comparable to H, as illustrated in Figure 2.13b.

Long-wavelength disturbances on either flank are not independent of each other and resonantly couple to form growing modes with zero phase speed. In particular, if $0 < kH \lesssim 0.64$, then the right-hand side of (2.144) is negative, meaning that ω is a pure imaginary number.

The fact that ω is complex-valued, means that the flow is unstable. To see this, suppose in general we have $\omega = \omega_r + \imath\sigma$. Substituting this into the formula for the streamfunction in (2.130) gives

$$\psi = \hat{\psi}(z)e^{\imath(kx-\omega_r t)}e^{\sigma t}. \tag{2.145}$$

Thus the real part of ω is the wave frequency and, if $\sigma > 0$, this is the growth rate of waves whose amplitude increases exponentially in time. The quantity $1/\sigma$ is known as the 'e-folding time'. Typically, the dispersion relation for ω is a polynomial with real coefficients. So if the roots are complex, they appear as complex-conjugate pairs. That is to say, if ω is complex, then an unstable solution with $\sigma > 0$ must exist.

Although there is no restriction to the wavenumber of allowable unstable waves, in reality the fastest growing solution is the one that is typically observed. From (2.144), the fastest growing mode, which is computed numerically, occurs for wavenumber $k^\star \simeq 0.398/H$, and the corresponding growth rate is $\sigma^\star \simeq 0.20 s_0$.

Recall that these predictions have been made under the assumption that the disturbances are small amplitude. So, although the unstable waves grow exponentially, they do not do so without bound. When their amplitude is sufficiently large, nonlinear effects become significant. In the case of the unstable shear layer, the waves grow and develop into coherent vortices sometimes called 'Kelvin–Helmholtz billows'. Eventually they turbulently break down.

Although linear theory cannot predict the long-time evolution of the flow, the wavelength of the most unstable mode sets the horizontal scale of the instability, even as it develops nonlinearly. Thus we expect the unstable shear layer to develop into a train of vortices separated approximately by $2\pi/k^\star \simeq 16H$.

2.6.4 Shear instability of interfacial waves

So far we have examined waves and instability in a fluid with uniform density. If in addition the system consists of layers of fluid with different density, then the system can support interfacial waves as well as Rayleigh waves. Density interfaces modify the interaction between pairs of Rayleigh waves in a Kelvin–Helmholtz unstable flow. They also lead to two new classes of instability. One is called 'Holmboe instability'. This results from the resonant coupling of an interfacial wave with a Rayleigh wave. The other class of instability has no generally accepted terminology, but will be referred to here as Taylor instability. This results from the resonant coupling of two interfacial waves mediated by a shear layer.

2.6.4.1 Kelvin–Helmholtz instability

First we examine how Kelvin–Helmholtz instability, examined in Section 2.6.3 for a uniform density fluid, is affected by the presence of density interfaces. Consider the shear layer given by (2.142) which moves in a three layer fluid with background density

$$\bar\rho = \begin{cases} \rho_1 & z \geq H \\ \frac{1}{2}(\rho_1 + \rho_2) & |z| < H \\ \rho_2 & z \leq -H \end{cases} . \tag{2.146}$$

For mathematical simplicity, this is set up so that density interfaces exist at the kinks of the shear profile and the density-jumps across each interface are equal.

The stability problem is solved by assuming the streamfunction amplitude has the form (2.143) but now the effect of discontinuity in the density profiles must be accounted for in the interface conditions (2.134) and (2.135).

After some algebra, the dispersion relation is given by the roots of the following quartic polynomial:

$$\tilde{\omega}^4 - \frac{1}{4}\left[8\tilde{k}^2 - 4(1-\mathrm{Ri}_b)\tilde{k} + 1 - e^{-4\tilde{k}}\right]\tilde{\omega}^2 + \frac{1}{4}\tilde{k}^2\left[(2\tilde{k} - 1 - \mathrm{Ri}_b)^2 - (1+\mathrm{Ri}_b)^2 e^{-4\tilde{k}}\right], \tag{2.147}$$

in which the frequency and wavenumber have been expressed nondimensionally by $\tilde{\omega} = \omega/s_0$ and $\tilde{k} = kH$.

In (2.147) we have introduced the bulk Richardson number defined by

$$\mathrm{Ri}_b \equiv \frac{g'/H}{{s_0}^2}, \tag{2.148}$$

in which $s_0 = U_0/H$ is the shear at mid-depth and $g' = g\frac{\rho_2-\rho_1}{(\rho_2+\rho_1)/2}$ is the reduced gravity. This is a characteristic measure of the way in which buoyancy forces may retard or overcome shear instability. Taking the limit $\mathrm{Ri}_b \to 0$ in (2.147), we recover the dispersion relation (2.144) as two of the roots.

Although the presence of density-jumps might be expected to stabilize the flow, it turns out that the flow is unstable even for large Ri_b. Larger density-jumps act to reduce the growth rate of the most unstable mode and to increase the corresponding wavenumber. For example, Figure 2.15a plots the frequency and growth rate as a function of wavenumber in the case $\mathrm{Ri}_b = 1$. This should be compared with the corresponding plot for the unstratified shear layer (for which $\mathrm{Ri}_b = 0$) shown in Figure 2.14.

Expecting that both ω_r and ω_i are zero at the conceptual boundary between stable and unstable modes, we find that coupled Rayleigh waves are unstable if their wavenumber k lies within a finite range of values given by

$$\frac{2kH}{1+\exp(-2kH)} - 1 < \mathrm{Ri}_b < \frac{2kH}{1-\exp(-2kH)} - 1. \tag{2.149}$$

The so-called 'marginal stability curves' given by (2.149) are plotted in the stability regime diagram shown in Figure 2.15b. In the limit $\mathrm{Ri}_b \to 0$, corresponding to a uniform-density fluid, the range of wavenumbers for which the flow is unstable is given by the values of kH for which the right-hand side of (2.144) is negative. The frequency and growth rate for modes in this case are plotted in Figure 2.14.

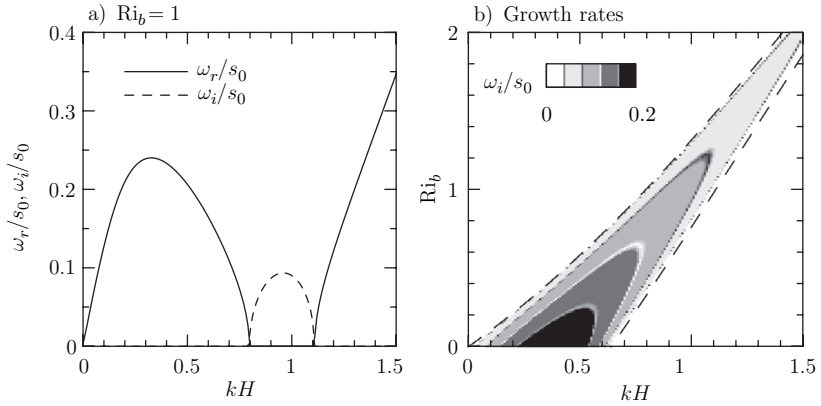

Fig. 2.15. a) Frequency (solid line) and growth rate (dashed line) versus wavenumber of modes associated with a piecewise-linear shear layer in a three-layer fluid whose middle-layer density is the average of the upper and lower layers. Values are computed for the bulk Richardson number $\mathrm{Ri}_b \equiv (g\Delta\rho/\rho_0)H/{U_0}^2 = 1$, in which ρ_0 is the characteristic density taken as the value of $\bar{\rho}$ at $z = 0$. b) Growth rates as they depend upon the wavenumber and Ri_b. The dashed lines indicate the marginal stability boundaries, given by (2.149). For large Ri_b, the most unstable mode has a nondimensional wavenumber $kH \simeq (\mathrm{Ri}_b + 1)/2$.

Corresponding to each eigenvalue, ω, is the eigenfunction $\hat{\psi}(z)$, which gives the structure of the Kelvin–Helmholtz modes. The z-dependence of $\hat{\psi}$ in each layer is given generally by (2.143) in which the coefficients $\mathcal{A}$, $\mathcal{B}_1$, $\mathcal{B}_2$ and C effectively form an eigenvector. Substituting ω for given k and Ri_b into the equations defining the interface conditions, one can explicitly solve for $\mathcal{A}$, $\mathcal{B}_1$ and C in terms of $\mathcal{B}_2$. The result can be normalized by setting $\mathcal{B}_2 = 1$.

Figure 2.16a shows the perturbation streamfunction amplitude computed in this way for the most unstable mode of the shear layer with $\mathrm{Ri}_b = 1$. Note that the function has real and imaginary parts as a consequence of $\omega = \imath 0.094 s_0$ being complex. To help interpret this result, Figure 2.16b shows greyscale contours of the perturbation streamfunction $\psi(x,z) = \Re\{\hat{\psi} e^{\imath kx}\}$. Here the amplitude and phase are established effectively by setting $t = 0$ and $\mathcal{B}_2 = 1$. At $x = 0$, ψ is identical to the real part of $\hat{\psi}$; at $x = 3/4\lambda$, $\psi(x,z)$ is identical to the imaginary part of $\hat{\psi}$. At other values of x the streamfunction is computed from $\hat{\psi}_r(z)\cos(kx) - \hat{\psi}_i(z)\sin(kx)$.

The structure of the growing instability is best illustrated by superimposing the perturbation streamfunction upon the background streamfunction $\bar{\psi}$, defined implicitly through $\bar{U} = -d\bar{\psi}/dz$. This is plotted in Figure 2.16d. Contours of the total streamfunction $\psi_T(x,z) = \bar{\psi}(z) + \epsilon\psi(x,z)$ are shown in Figure 2.16e. Here, the amplitude of the perturbation is established through the choice of ϵ. As time progresses, the amplitude grows exponentially as $\exp(\omega_i t)$. Thus we see that the

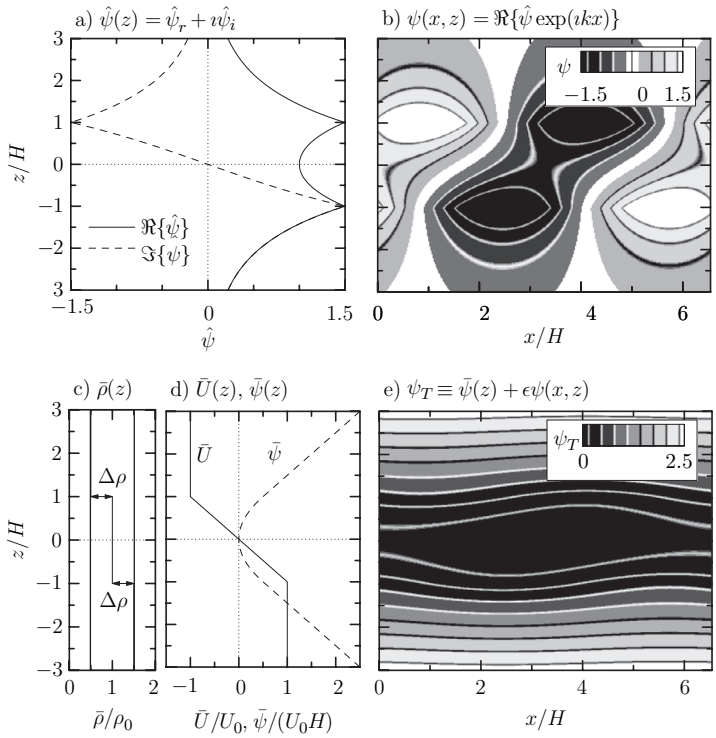

Fig. 2.16. a) Vertical structure of the perturbation streamfunction amplitude for an unstable disturbance in a shear layer with density interfaces at $z = \pm H$. It is computed for the most unstable mode in the case $\mathrm{Ri}_b = 1$, for which $k^\star H = 0.96$ and $\omega/s_0 \simeq \imath 0.094$. The eigenfunction is normalized so that $\hat{\psi}(0) = 1$. b) Corresponding spatial structure of the perturbation streamfunction $\psi(x,z) = \Re\{\hat{\psi}\exp(\imath kx)\} = \Re\{\hat{\psi}\}\cos(kx) - \Im\{\hat{\psi}\}\sin(kx)$. Background profiles of c) density and d) velocity (solid line) and streamfunction (dashed line), the latter being defined by $\bar{U} = -d\bar{\psi}/dz$. e) Contours of the total streamfunction $\psi_T = \bar{\psi} + \epsilon\psi$ in which the amplitude of the perturbation has been taken as $\epsilon = 0.1$.

instability distorts the streamlines, pulling them apart near the centre of the shear layer between $x = \lambda/4$ and $3\lambda/4$.

The waves grow by extracting energy from the background shear flow. The growth rate decreases as the density-jump across the interfaces (measured by Ri_b) becomes larger because some of the kinetic energy extracted must go into the available potential energy associated with the disturbance.

As the instability grows to very large amplitude, the linear theory approximations used to derive the form of the disturbance are no longer valid. Nonlinear simulations show that the disturbance saturates at finite amplitude if Ri_b is sufficiently large. In weak stratification however, the contours can wrap up to form a vortex centred in the middle of the shear layers.

2.6.4.2 Holmboe instability

Next we examine Holmboe waves. Generally, these occur when the density interface is not coincident with the change in shear. In this piecewise-linear problem it is necessary for the interface to be embedded within the shear in order for instability to occur. Explicitly, we consider the kinked shear profile given by (2.138) and we now suppose this is a two-layer fluid with a density interface at $z = -H < 0$:

$$\bar{\rho} = \begin{cases} \rho_1 & z \geq -H \\ \rho_2 & z < -H \end{cases} . \tag{2.150}$$

Solving (2.133) with interface conditions (2.134) and (2.135), we find that the waves must satisfy the dispersion relation

$$\tilde{\omega}^3 - \left(2\tilde{k} + \frac{1}{2}\right)\tilde{\omega}^2 + \tilde{k}\left(\tilde{k} + 1 - \frac{1}{2}\mathrm{Ri}_b\right)\tilde{\omega} - \frac{1}{2}\tilde{k}\left(\tilde{k} - \frac{1}{2}\mathrm{Ri}_b\left[1 - e^{-2\tilde{k}}\right]\right) = 0, \tag{2.151}$$

in which $\tilde{\omega} \equiv \omega/s_0$, $\tilde{k} \equiv kH$, and we have defined the bulk Richardson number as in (2.148), but with $g' \equiv g(\rho_2 - \rho_1)/\rho_0$, in which ρ_0 is the characteristic density, which can be taken to equal ρ_2. The definitions of Ri_b are the same in the Boussinesq limit.

In uniform fluid, $\mathrm{Ri}_b = 0$ and so the cubic polynomial on the left-hand side of (2.151) has one root $\tilde{\omega} = 1/2$, corresponding to the dispersion relation for Rayleigh waves (2.141). The remaining double root is $\tilde{\omega} = -\tilde{k}$. For finite Ri_b, this double root introduces a new class of disturbance that evolves due to interfacial waves at $z = -H$ interacting with Rayleigh waves centred near $z = 0$. For a range of k, these double-roots are complex-valued, meaning that the coupling between the two types of waves renders them unstable. The complex dispersion relation is plotted for the case $\mathrm{Ri}_b = 1$ in Figure 2.17a. The thick solid line in the figure also shows the phase speed $c_p = \omega_r/k$.

Unlike shear instability, whose dispersion relation is given by the roots of (2.144), the complex roots of (2.151) have non-zero real as well as imaginary parts. Thus Holmboe waves are not stationary, but as they grow they also propagate in the direction of the shear flow below $z = 0$. This is a distinguishing feature of Holmboe waves.

The values of kH and Ri_b that result in unstable waves are shown in Figure 2.17b. Consistent with our analysis, we see that the growth rate is zero if $\mathrm{Ri}_b = 0$, meaning that there is no density interface. Instability occurs even for very small Ri_b with the most unstable mode having a wavenumber that increases as Ri_b increases. The growth rate is fastest if $\mathrm{Ri}_b \simeq 0.56$, in which case the most unstable mode has a nondimensional wavenumber $kH \simeq 0.89$ and growth rate $\omega_i = 0.14 s_0$.

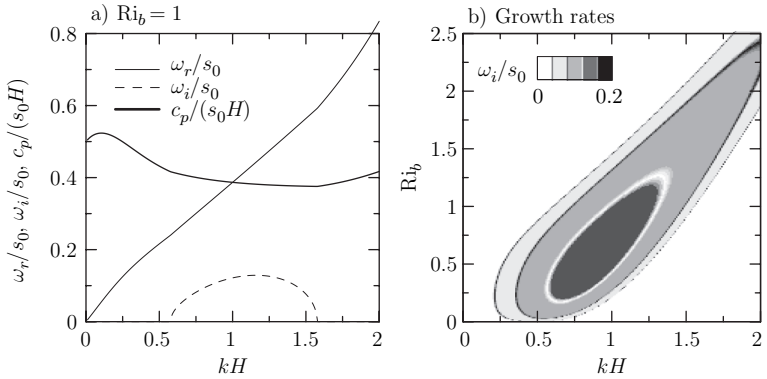

Fig. 2.17. Frequency (ω_r, solid line) and growth rate ($\omega_i \equiv \sigma$, dashed line) of the Holmboe instability resulting from a density interface lying a distance H above a kinked-shear profile with shear s_0 below $z = 0$. The results are plotted for the complex roots of (2.151) with the positive imaginary part for the case with $\mathrm{Ri}_b = 1$.

The structure of the most unstable mode in the case $\mathrm{Ri}_b = 1$ is shown in Figure 2.18. Unlike the corresponding Kelvin–Helmholtz mode shown in Figure 2.16, the Holmboe mode has a cusped structure that peaks near the kink of the shear profile. As time progresses, this mode grows in amplitude and propagates rightwards.

In many laboratory and geophysical circumstances Holmboe waves are created by a finite-depth shear layer in which the density interface is offset from the midpoint of the shear. In this case Holmboe waves appear on the upper and lower flanks of the shear layer. Their presence is distinguished from Kelvin–Helmholtz instability by the appearance of leftward- and rightward-propagating waves on either flank of the shear layer. Whereas Kelvin–Helmholtz waves have the same speed as the midpoint of the shear and wrap into vortices as they develop nonlinearly, finite-amplitude Holmboe waves form cusps that move in opposite directions above and below the shear layer. The cusps are more pronounced on one flank if the interface is closer to the kink in the shear profile on that flank.

2.6.4.3 Taylor instability

Finally, we examine the circumstance in which two interfacial waves interact through a uniform shear flow. Explicitly, we consider the circumstance in which the background flow is given by

$$\bar{U} = -s_0 z \tag{2.152}$$

for all z, and the three-layer density profile is given by (2.146).

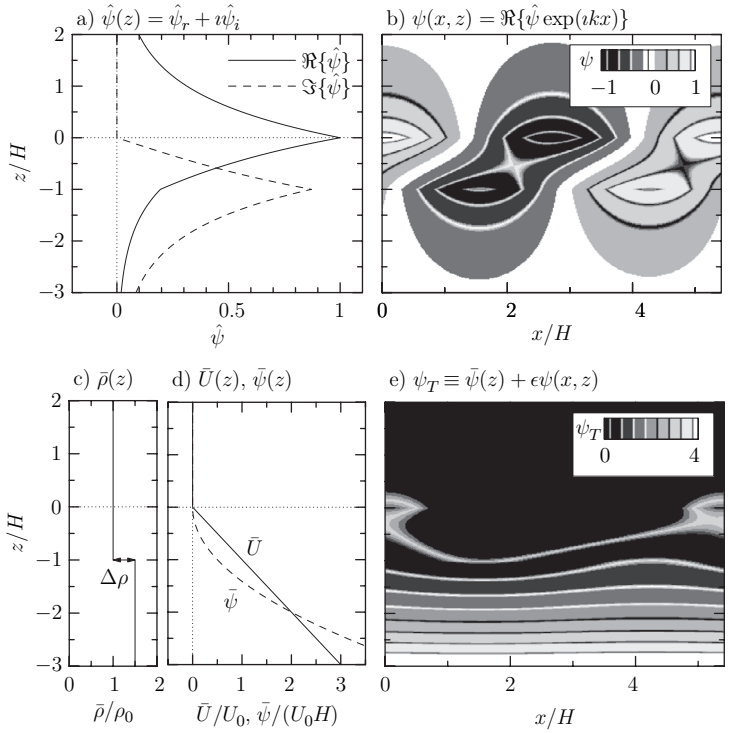

Fig. 2.18. As in Figure 2.16 but showing the structure of the most unstable Holmboe mode in a kinked-shear flow with a density interface at $z = -H$. The functions are computed for the case $\mathrm{Ri}_b = 1$, in which circumstance the most unstable mode has a wavenumber $k^\star H = 1.16$ and complex frequency $\omega/s_0 \simeq 0.443 + \imath 0.129$. a) Vertical structure of the perturbation streamfunction amplitude function $\hat{\psi}(z)$, b) the corresponding spatial structure of the perturbation streamfunction, background profiles of c) density and d) velocity (solid line) and streamfunction (dashed line), and e) contours of the total streamfunction $\psi_T = \bar{\psi} + \epsilon\psi$ in which $\epsilon = 0.3$.

Again we take the streamfunction amplitude to have the form (2.143). For mathematical simplicity we assume the fluid is Boussinesq and so apply the interface conditions (2.134) and (2.137). Thus we find the dispersion relation is given by the roots of

$$\tilde{\omega}^4 - \tilde{k}\left(2\tilde{k} + \mathrm{Ri}_b\right)\tilde{\omega}^2 + \frac{1}{4}\tilde{k}^2\left[(2\tilde{k} - \mathrm{Ri}_b)^2 - {\mathrm{Ri}_b}^2\exp(-4\tilde{k})\right] = 0. \qquad (2.153)$$

Here $\tilde{\omega} \equiv \omega/s_0$, $\tilde{k} \equiv kH$ and the bulk Richardson number is given by (2.148).

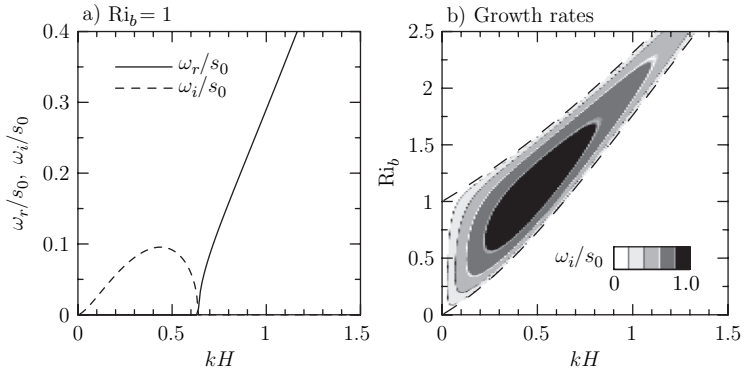

Fig. 2.19. As in Figure 2.15 but showing the dispersion relation associated with a Taylor mode in a uniform shear flow with a three-layer density profile whose middle-layer density is the average of the upper and lower layers. a) Frequency (solid line) and growth rate (dashed line) versus wavenumber of modes computed in the case $\mathrm{Ri}_b = 1$. b) Growth rates as they depend upon the wavenumber and Ri_b. The dashed lines indicate the marginal stability boundaries, given by (2.154).

The roots of (2.153) are complex and the flow unstable if

$$\frac{2\tilde{k}}{1+\exp(-2\tilde{k})} < \mathrm{Ri}_b < \frac{2\tilde{k}}{1-\exp(-2\tilde{k})}. \tag{2.154}$$

These stability boundaries are indicated by the dashed lines in Figure 2.19b. In a shear flow with no density interfaces ($\mathrm{Ri}_b = 0$), no instability occurs. Like Kelvin–Helmholtz modes, the frequency (and hence phase speed) of the disturbances is zero if the mode is unstable. Here, however, the fastest growing modes generally have a much smaller wavenumber and correspondingly larger horizontal and vertical extents.

The structure of the most unstable mode in the case $\mathrm{Ri}_b = 1$ is shown in Figure 2.20. This is qualitatively similar to the structure of Kelvin–Helmholtz modes but it must be kept in mind that there is no kink in the shear flow and so the dynamics driving the instability are fundamentally different. The presence of shear allows interfacial waves in a three-layer fluid to grow in amplitude through extracting kinetic energy from the background shear.

2.7 Interfacial waves influenced by rotation

The Earth's rotation is important for waves having periods longer than many hours and typically on the order of days. Such waves also tend to be of broad horizontal extent – so wide that shallow water theory may be applied.

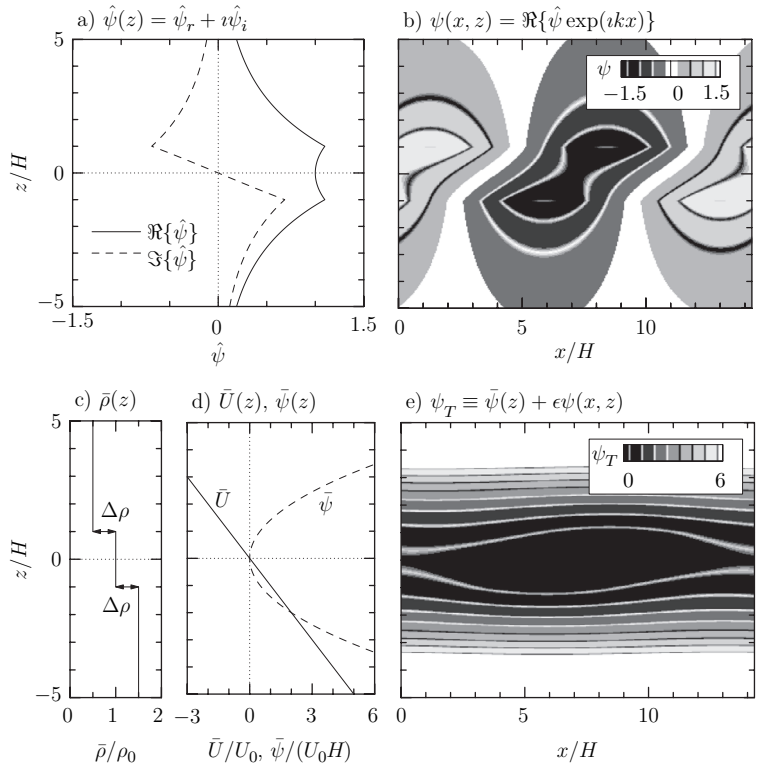

Fig. 2.20. As in Figure 2.16 but showing the structure of the most unstable Taylor mode in a uniform shear flow with density interfaces at $z = \pm H$. The functions are computed for the case $\mathrm{Ri}_b = 1$, in which circumstance the most unstable mode has a wavenumber $k^\star H = 0.44$ and growth rate $\omega_i/s_0 \simeq 0.096$. a) Vertical structure of the perturbation streamfunction amplitude function $\hat{\psi}(z)$, b) the corresponding spatial structure of the perturbation streamfunction, background profiles of c) density and d) velocity (solid line) and streamfunction (dashed line), and e) contours of the total streamfunction $\psi_T = \bar{\psi} + \epsilon\psi$ in which $\epsilon = 0.3$.

For this reason, here we present the theory for waves in a two-layer shallow water fluid in which buoyancy is felt through the reduced gravity $g' = g(\rho_2 - \rho_1)/\rho_2$, and the equivalent depth is the harmonic mean of the upper and lower layer depths (2.99): $\bar{H} = H_1H_2/(H_1 + H_2)$.

A shallow water two-layer fluid describes interfacial waves that are long compared with the depth of the upper and lower layer fluids, as would be the case for long oceanic waves at the thermocline.

A shallow water one-and-a-half-layer fluid, recovered in the limit $\bar{H} \to H$, represents waves moving along an interface that separates a relatively thin slab of fluid from an effectively infinitely deep fluid layer. This might describe long-wavelength